Comparison of gonadal toxicity of single fraction ultra-high dose rate and conventional radiation in mice

Maria C. Cuitiño DVMPhD , Jessica L. Fleming PhD , Sagarika Jain MS , Ashley Cetnar PhD , Ahmet S. Ayan PhD , Jeffrey Woollard PhD , Heather Manring PhD , Wei Meng PhD , Joseph P. McElroy PhD , Dukagjin M Blakaj MDPhD , Nilendu Gupta PhD , Arnab Chakravarti MD

PII: S2452-1094(23)00030-1
DOI: https://doi.org/10.1016/j.adro.2023.101201
Reference: ADRO 101201

To appear in: *Advances in Radiation Oncology*

Received date: 3 November 2022
Accepted date: 8 February 2023

Please cite this article as: Maria C. Cuitiño DVMPhD , Jessica L. Fleming PhD , Sagarika Jain MS , Ashley Cetnar PhD , Ahmet S. Ayan PhD , Jeffrey Woollard PhD , Heather Manring PhD , Wei Meng PhD , Joseph P. McElroy PhD , Dukagjin M Blakaj MDPhD , Nilendu Gupta PhD , Arnab Chakravarti MD , Comparison of gonadal toxicity of single fraction ultra-high dose rate and conventional radiation in mice, *Advances in Radiation Oncology* (2023), doi: https://doi.org/10.1016/j.adro.2023.101201

Title: Comparison of gonadal toxicity of single fraction ultra-high dose rate and conventional radiation in mice

Short Running Title: Gonadal toxicity of ultra-high dose rate radiation

Maria C. Cuitiño, DVM, PhD[1], Jessica L. Fleming, PhD[1], Sagarika Jain, MS[1], Ashley Cetnar, PhD[1], Ahmet S. Ayan, PhD[1], Jeffrey Woollard, PhD[1], Heather Manring, PhD[1], Wei Meng, PhD[1], Joseph P. McElroy, PhD[2], Dukagjin M Blakaj, MD, PhD[1], Nilendu Gupta, PhD[1], and Arnab Chakravarti, MD[1]

[1]Department of Radiation Oncology, Arthur G. James Hospital, Comprehensive Cancer Center, [2]Department of Biomedical Informatics, Center for Biostatistics, The Ohio State University, Columbus, Ohio, USA

Corresponding Author Information:
Arnab Chakravarti
Arnab.Chakravarti@osumc.edu

Author Responsible for Statistical Analysis:
Joseph McElroy
Joseph.McElroy@osumc.edu

Conflict of Interest:
Arnab Chakravarti reports a relationship with Varian Medical Systems that includes: funding grants. Dukagjin Blakaj reports a relationship with IntraOp Medical that includes: funding grants. Ashley Cetnar reports a relationship with AAPM Rocky Mountain Chapter Meeting that includes: travel reimbursement. Ashley Cetnar reports a relationship with American Association of Physicist in Medicine that includes: board membership. Joseph P. McElroy reports a relationship with The Ohio State University Department of Radiation Oncology that includes: employment and non-financial support. Jessica Fleming serves as Associate Senior Editor for Advances in Radiation Oncology. Ahmet Ayan serves as Associate Section Editor for Advances in Radiation Oncology.
No other potential conflicts of interest were reported.

Funding:
This work was supported by the grants R01CA108633, R01CA169368, RC2CA148190, U10CA180850-01 (NCI) and the Ohio State University CCC (all to A. Chakravarti).

Data Availability:
Research data are stored in an institutional repository and will be shared upon request to the corresponding author.

Acknowledgements:

We thank Johanna Rawlings and Kevin Thorburn for assistance with histology and immunohistochemistry. This work was supported by the Comparative Pathology and Digital Imaging Shared Resource (CPDISR) at The Ohio State University.

ABSTRACT

Purpose

Increasing evidence suggests that ultra-high dose rate (UHDR) radiation could result in similar tumor control as conventional (CONV) radiotherapy (RT) while reducing toxicity to surrounding healthy tissues. Considering that radiation toxicity to gonadal tissues can cause hormone disturbances and infertility in young cancer patients, the purpose of this study was to assess the possible role of UHDR-RT in reducing toxicity to healthy gonads in mice as compared to CONV-RT.

Methods and Materials

Radiation was delivered to the abdomen or pelvis of female (8 or 16 Gy) and male (5 Gy) C57BL6 mice, respectively, at conventional (~0.4 Gy/s) or ultrahigh (>100 Gy/s) dose rates using an IntraOp Mobetron linear accelerator. Organ weights along with histopathology and immunostaining of irradiated gonads were used to compare toxicity between radiation modalities.

Results

CONV- and UHDR-RT induced a similar decrease in uterine weights at both studied doses (~50% of controls), which indicated similarly reduced ovarian follicular activity. Histologically, ovaries of CONV- and UHDR-irradiated mice exhibited a comparable lack of follicles. Weights of CONV- and UHDR-irradiated testes were reduced to ~30% of

controls, and the percent of degenerate seminiferous tubules was also similar between radiation modalities (~80% of controls). Pairwise comparisons of all quantitative data indicated statistical significance between irradiated (CONV or UHDR) and control groups (from P Ò0.01 to P Ò0.0001) but not between radiation modalities.

Conclusions

The data presented here suggest that the short-term effects of UHDR-RT on the mouse gonads are comparable to those of CONV-RT.

INTRODUCTION

Ionizing radiation is an effective treatment for cancer, but its curative potential is limited by a variety of acute and late toxic effects on normal tissues.[1] FLASH radiotherapy (FLASH-RT), which is defined as ultra-high dose rate (UHDR-RT) (>40 Gy/s) radiation, has been recently shown to result in reduced toxicity to healthy tissues while maintaining similar tumor control as conventional (CONV)-RT (~0.1 Gy/s) in preclinical models.[2] Thus, the use of FLASH-RT could lead to an increase in therapeutic ratio with greater potential for tumor control. The in vivo biological response of normal tissue sparing is referred to as ñthe FLASH effectòand has been reported mostly using electron and proton beams.[2,3] The molecular mechanisms underlying this observed protective effect are largely unknown, but proposed mechanisms include differential regulation of pro- and anti-inflammatory molecules, DNA damage and repair, apoptosis and senescence to list a few.[4]

The existing preclinical data uniformly support the notion that FLASH-RT provides comparable tumor control as CONV-RT, although the evidence concerning the proposed reduced toxicity of FLASH on normal tissues is less compelling. Most observations to date are derived from mouse studies using moderately radiosensitive tissues, namely the brain, the lung and the skin.[5ï12] Fewer studies have focused on highly sensitive and acutely responding tissues such as the gastrointestinal tract and the hematopoietic system.[13ï15] Despite a growing body of evidence pointing to the existence of a ñFLASH effectò, conflicting data continue to emerge as a number of studies have failed to demonstrate sparing across different systems, tissues and species.[16ï21] Discrepancies in study results have been attributed to a lack of homogeneity on the irradiation beam parameters used across experiments, and recommendations on standards for uniformly reporting physical aspects of FLASH have been made to contribute to alleviate this issue.[22]

Male and female germ cells are among the most radiation sensitive cell types in the body.[23,24] Radiation therapy can injure gonadal tissues and result in significant morbidities in young cancer patients.[25] In addition to male and female infertility and the detrimental consequences of premature ovarian failure in women, endocrine dysfunction can impair proper sexual development in prepubertal children undergoing treatment for hematologic malignancies.[26] Given the general lack of preclinical studies assessing a possible protective role of FLASH-RT on healthy gonads, the present study was conducted to evaluate the effects of a single fraction of UHDR-RT as compared to CONV-RT on the mouse female and male reproductive organs as models of acute radiation injury. Intriguingly, analysis of organ weights along with thorough histopathological and

immunohistochemical evaluation of irradiated tissues suggested that the short-term effects of UHDR-RT on the mouse gonads are comparable to those of CONV-RT.

METHODS

Mouse models and care

Mouse usage was approved by the Institutional Animal Care and Use Committee at The Ohio State University. C57BL/6 mice were purchased from The Jackson Laboratory at 6 weeks of age and allowed to acclimate for a minimum of two weeks prior to irradiation. Mice were housed under normal husbandry conditions (five or less animals per cage) in a vivarium with a 12-hour light/dark cycle. For high dose abdominal irradiation, body weight and overall health condition were assessed by applying the MISS 3 scoring system following recommended removal criteria.[27]

Mouse irradiation

Adult (2 to 4-month-old) C57BL/6J mice were irradiated at both UHDR and CONV dose rates using an Mobetron (IntraOp, Sunnyvale, CA) linear accelerator. Detailed information on irradiation beam parameters is presented in Supplementary Table 1. Mice were anesthetized with isoflurane in air and positioned supine in a custom 3D printed PLA plastic immobilization device (Figure 1A-B). A 6 mm thick, 3.5x4 cm (length x width) copper collimator was used to target radiation to the abdominal (female) and pelvic (male) regions (Figure 1A and C). For abdominal irradiation in female mice, the xiphoid process

of the sternum was used to mark the cranial end of the irradiation field (Figure 1B). For pelvic irradiation in male mice, the scrotal area was placed in the center of the irradiation field (Figure 1B). Gafchromic EBTXD (Ashland Advanced Materials, Bridgewater NJ) films were placed beneath the irradiated region for dosimetry and the exit dose was recorded for each mouse (Figure 1D and Supplementary Table 1). Percent depth dose as well as lateral and longitudinal dose profiles at depth of maximum dose (d_{max}) were acquired using GafChromic film in Solid Water phantom slabs (Figure 1E).

Irradiation machine and setup

The Mobetron is a mobile electron linear accelerator capable of delivering 9 MeV electrons at conventional dose rates of the order of ~10 Gy/min as well as UHDRs greater than 40 Gy/s. Two different SSD configurations were used in the irradiations, with collimator placement at 2 or 35 cm below the exit window of the linac (Conf2 and Conf35, respectively), as shown in Figure 1C. The Mobetron delivers UHDR radiation at discrete combinations of pulse width (PW), pulse repetition frequency (PRF) and number of pulses. The dose and dose rate in the UHDR realm are not independent parameters, and only a discrete set of doses and dose rates can be achieved using a particular collimator and SSD configuration. Percent depth doses (PDD), dose profiles and dose at d_{max} were obtained through film dosimetry in solid water for both energies at the two SSD configurations. The UDHR data is measured at 60 Hz PRF and 4 us pulse width, and correction factors are applied to the dose per pulse when changing PRF and PW to obtain the intended dose and dose rate. The setup parameters used for the three sets of

experiments included in this study are outlined in Supplementary Table 1. Representative PDD and profile data are shown in Figure 1E.

Approach to the analysis of ovarian toxicity

Given that counting ovarian follicle numbers accurately can be challenging, the quantitative assessment of radiation-induced ovarian follicle loss in this study was performed indirectly by measuring changes in uterine weight.[28,29] In mice undergoing normal estrus cycles, late tertiary ovarian follicles secrete estradiol which causes cyclical increases in uterine weight. Radiation induced loss of ovarian follicles is expected to lead to reduced estradiol levels and subsequent decreases in uterine weight that manifest with variable latency depending on the radiation dose delivered. Qualitative assessment of ovarian follicle damage was performed histologically as well as by immunohistochemistry (see ñhistopathological analysesò section for details on classification of follicles). Ovarian follicle sensitivity to radiation varies depending on the follicleôs maturation stage.[30] In this study, a dose Ó16 Gy induced immediate (within days) degeneration and loss of all follicle stages including existing late tertiary follicles. Thus, changes in uterine weight at this dose were noticeable within a few days after irradiation. Day 6 post-irradiation was defined as the endpoint for this dose as mice receiving 16 Gy experience GI syndrome and meet early removal criteria around this time. In contrast, a dose Ò8 Gy caused immediate loss of small follicles while preserving existing (secondary and tertiary) follicles with no immediate changes in uterine weights. Thus, this dose was used to study radiation induced loss of small follicles. Uterine weights were evaluated 2 months after irradiation at this dose based on follicular maturation time (from primordial to late tertiary), which is

estimated to be about 1.5 months in mice. Under this premise, a latency period of at least two months would be sufficient for small follicles surviving 8 Gy to grow into tertiary follicles and exert estrogenic influence on the uterus.[31,32] For all experiments, fresh uterine weights were recorded at necropsy and are presented as percent of body weight except for 16 Gy. Weight loss occurs acutely at the latter dose making comparison to unirradiated controls less reliable and thus uterine weight data are presented in milligrams instead.

Approach to the analysis of testicular toxicity

Testicular weights were used as a readout of radiation-induced toxicity. Due to the exquisite sensitivity of germ cells to radiation, a dose of 5 Gy was chosen for these experiments in order to allow for survival of at least a subset of spermatogonia and subsequent evaluation of tubular repopulation.[33,34] The endpoint for assessing radiation toxicity on testicular germ cells was set at 35 days post-irradiation as it takes mouse spermatogonia ~35 days to mature into spermatozoa and achieve some level of restitution of the seminiferous epithelium.[35] For all experiments, fresh testis weights were recorded at necropsy and are presented as percent of body weight. The testis and epididymis were subjected to histopathological evaluation. The percent of seminiferous tubules exhibiting degeneration was used as additional quantitative evidence of radiation-induced testicular toxicity (see histopathological analyses).

Tissue preparation and histology

Tissue used for histology was fixed with 10% pH-buffered formalin (Fisher Scientific; 23-245-685) for 48-72 hours at room temperature, embedded in paraffin and cut into 4 εm sections for staining with hematoxylin and eosin (H&E).

Histopathological analyses

Ovarian toxicity

Histopathological evaluation of ovaries and uteri was performed by a board-certified veterinary pathologist (MCC) following recommended nomenclature.[36] Ovarian follicle damage was evaluated qualitatively on representative middle sections of ovaries stained with H&E, which was complemented by IHC staining with an oocyte marker (MVH) to highlight the presence or absence of oocytes within follicles. Follicle stages were identified according to morphological criteria as primordial (oocyte surrounded by a single layer of flattened pre-granulosa cells), primary (oocyte surrounded by a single layer of cuboidal to columnar granulosa cells), secondary (two or more layers of granulosa cells, and a zona pellucida between oocyte and granulosa cells), tertiary (multiple layers of granulosa cells and small antrum) and late tertiary follicles (large antrum, oocyte and corona radiata are no longer attached to the wall of the follicle).[36] In this study, primordial and primary follicles are also collectively referred to as small follicles whereas secondary and tertiary follicles are referred to as medium/large follicles. The histomorphology of the uterus is dependent on hormonal changes and can be correlated with specific phases of the estrus cycle and cycle abnormalities in rodents.[37] These histological features were

used in this study as additional evidence of radiation-induced ovarian toxicity to facilitate comparisons between CONV and UHDR-irradiated mice.

Testicular toxicity

The testis and epididymis were subjected to histopathological evaluation by a board-certified veterinary pathologist (MCC) following standard nomenclature.[38] Quantification of the percent of degenerate seminiferous tubules was done using micrographs of H&E-stained sections. Tubules exhibiting an intact epithelium containing spermatogonia, spermatocytes and spermatids were counted as non-degenerate. Sertoli cell-only tubules (tubules completely lacking germ cells) as well as tubules exhibiting partial depletion of germ cells, degenerating or apoptotic germ cells, or Sertoli cell cytoplasmic vacuolation were classified as degenerate.[38] The percent of degenerate tubules was estimated from observing at least 120-150 tubules per mouse.

Immunostaining

Immunostaining was performed using a ThermoScientific Lab Vision Autostainer 360 as per manufacturerôs instructions. Briefly, a citrate-based solution (Dako S1699) was used for epitope retrieval at ~95°C in a steamer for 20 minutes. A 3% H2O2/PBS solution was used for endogenous enzyme block. Once in the autostainer, slides were incubated with 2.5% normal horse serum for 20 minutes, then incubated with rabbit anti-MVH (abcam, Ab13840) diluted to 1ug/mL in Dako Antibody Diluent (Dako S3022) for 30 minutes, rinsed, and then incubated with ImmPRESS Horse Anti-Rabbit HRP (Vector Laboratories MP-7401) for 30 minutes. DAB (Dako K3468) was applied for 2.5 minutes.

Statistical analysis

Studentôs t-test was used for pairwise comparisons of mean organ weights and percent testicular degeneration. GraphPad Prism version 9.2.0 (332) for Windows, GraphPad Software, LCC was used for analysis. A p-value less than 0.05 was considered statistically significant.

RESULTS

8 Gy UHDR-RT delivered in one single pulse induces similar acute ovarian toxicity as CONV-RT

To evaluate the level of toxicity of UHDR-RT on the ovary as compared to CONV-RT, C57BL/6J mice were anesthetized and positioned supine in a custom 3D printed PLA plastic immobilization device. The abdomen was placed in the center of a 3.5x4 cm^2 irradiation field using a copper collimator (Figure 1A-C). An IntraOp Mobetron linear accelerator was used to deliver radiation at both UHDR and CONV dose rates (Figure 1C-E). We initially evaluated the impact of a dose of 8 Gy on small ovarian follicles when delivered in a single pulse at UHDR (2.31E+06 Gy/s) or CONV (0.436 Gy/s) dose rates. Detailed information on irradiation beam parameters is presented in Supplementary Table 1. Radiation to the ovary is expected to cause loss of ovarian follicles. The quantitative assessment of radiation-induced ovarian follicle loss in this study was performed indirectly by measuring changes in uterine weight as the uterus responds to estradiol secreted by active ovarian follicles. A detailed description of the experimental approach to the analysis

of ovarian toxicity, including the rationale for determining endpoints to measure uterine weights according to radiation dose, is provided in methods. Mice were euthanized 2 months post-irradiation (PI), fresh uterine weights were recorded, and the reproductive tract was subjected to histopathological evaluation. On gross examination of the uterus, both UHDR and CONV irradiated mice exhibited slightly elongated uterine horns, which appeared smaller in diameter than control horns (Figure 2A). Uterine weights of both UHDR and CONV-irradiated mice were decreased to ~50% of control mice, which suggested comparably reduced ovarian follicle activity (Figure 2B). UHDR and CONV irradiated uteri exhibited histological features of reduced ovarian follicular activity, namely a narrow lumen and an endometrium lined by low columnar epithelium (Figure 2C). Features of estrogenic stimulation such as luminal dilatation were only observed in control mice (Figure 2C). In agreement with these findings, the ovaries of both UHDR and CONV irradiated mice lacked follicles of all types (see methods for classification of ovarian follicles) and were primarily composed of sheets of round cells reminiscent of ovarian interstitial cells (Figure 2D). Immunohistochemistry for the mouse vasa homologue (MVH) protein, a germ cell marker expressed in the cytoplasm of oocytes, highlighted the lack of oocytes within follicles in middle sections of ovaries (Figure 2E). The absence of tertiary ovarian follicles two months after a dose of 8 Gy was interpreted to be the result of acute radiation toxicity to small follicles (see methods for details on timing of follicular maturation). Late tertiary follicles are the source of estrogen and their absence in irradiated ovaries explains the reduced uterine weights and accompanying histological features of reduced estrogenic stimulation. Taken together, these findings suggest that

the acute toxic effects of single pulse UHDR-RT on the adult mouse ovaries are similar to those of CONV-RT.

16 Gy UHDR-RT delivered in multiple pulses induces similar acute ovarian toxicity as CONV-RT

To evaluate the toxic effect of UHDR-RT on ovarian follicles when delivered in multiple pulses, 16 Gy was given to the abdomen of C57BL/6J female mice in UHDR (234 Gy/s) or CONV (0.436 Gy/s) dose rate modes as previously described. Detailed information on irradiation beam parameters is presented in Supplementary Table 1. All mice were euthanized 6 days PI (see methods for description of the experimental approach and determination of endpoints for evaluation of the reproductive organs). No difference in the percent of body weight loss was observed between irradiated groups (~22-25% of baseline at day 6). Fresh uterine weights were recorded, and ovaries and uteri were subjected to histopathological evaluation. Upon gross examination, all irradiated uteri, regardless of the modality, were reduced in size and appeared thinner than control uteri (Figure 3A). Uterine weights of both UHDR and CONV-irradiated mice were decreased to ~50% of control mice, suggesting similarly reduced ovarian activity compared to unirradiated uteri (Figure 3B). As expected from these findings, all irradiated uteri exhibited histological features of reduced ovarian follicular activity, such as a narrow lumen lined by cuboidal epithelial cells (Figure 3C). In agreement with these findings, histological analysis of ovaries of UHDR and CONV irradiated mice demonstrated a lack of intact follicles (including tertiary follicles) and corpora lutea (Figure 3D). In contrast to control ovaries, only remnants of degenerate medium to large follicles were recognized

in UHDR and CONV-irradiated ovaries. Follicle remnants were composed of viable or degenerate oocytes lacking surrounding granulosa cells (Figure 3D). Signs of degeneration observed in oocytes were nuclear pyknosis or karyorrhexis, hypereosinophilic cytoplasm, and/or cytoplasmic fragmentation (Figure 3D). Immunohistochemistry for MVH highlighted oocytes within degenerate medium-large follicle remnants as well as the absence of small follicles (Figure 3E). Small degenerate corpora lutea composed of vacuolated cells were also observed (Figure 3D). Overall, these acute ovarian changes were indistinguishable between UHDR and CONV irradiated mice. In addition to depleting the more radiation-sensitive small follicles, this dose acutely damaged mature follicles which resulted in immediate reduction of uterine weights and accompanying histological features of reduced estrogenic stimulation in all irradiated mice. Taken together, these results suggest that high dose, UHDR-RT delivered in multiple pulses induces similar acute ovarian toxicity as CONV-RT.

5 Gy UHDR-RT delivered in a single pulse induces similar acute testicular toxicity as CONV-RT

To evaluate the impact of UHDR-RT on testicular germ cells when delivered in a single, 5 Gy were delivered to the pelvis of adult mice in UHDR (2.35E+06 Gy/s) or CONV (0.436 Gy/s) dose rate modes (Supplementary Table 1). To this end, the scrotal region of mice was placed in the center of a 3.5x4 cm irradiation field using a copper collimator as described for female mice (Figure 1B). Mice were euthanized 35 days PI, testicular weights were recorded, and the testes and epididymides were subjected to histopathological evaluation (see methods for description of the experimental approach

and determination of endpoints). On gross examination, the testes of CONV and UHDR irradiated mice were significantly smaller than those of control mice, and testis weight was reduced to ~30% of control mice for both modalities (Figure 4A-B). Histologically, testis of CONV and UHDR irradiated mice exhibited widespread germ cell degeneration and loss (Figure 4C). No sperm was observed in the epididymis of mice in either of the irradiated groups (Figure 4C), indicating that spermatogenesis was similarly reduced. Immunostaining of testis sections for the MVH protein, a germ cell marker expressed in the cytoplasm of spermatogonia and spermatocytes, highlighted the marked, general reduction in the number of germ cells in all irradiated testes (Figure 4D). In agreement with organ weight, the percent of degenerate tubules was strikingly similar (~80%) between UHDR and CONV irradiated mice (Figure 4E), indicating that the acute toxic effects of UHDR-RT on spermatogenic cells at the studied dose and dose rate are comparable to those induced by CONV-RT.

DISCUSSION

The proposed normal tissue sparing effect of FLASH-RT has generated great interest among radiation scientists as the number of preclinical studies assessing this intriguing phenomenon continues to increase. Radiation injury to gonadal tissues can result in significant morbidities in young cancer patients and therefore a possible role of UHDR-RT in protecting healthy gonads carries great translational impact.[39] To assess this possibility and to extend the existing data on FLASH-RT on acutely responding tissues, the present study evaluated the effects of a single fraction of electron radiation at UHDRs as compared to conventional DRs on the mouse female and male gonads. Analysis of

organ weights along with histopathological and immunohistochemical evaluation of irradiated tissues demonstrated that the short-term effects of UHDR-RT on the mouse gonads are comparable to those of CONV-RT.

Several levels of biological evidence are provided in this study that demonstrate similar gonadal toxicity between UHDR-RT and CONV-RT. Different parts of the female reproductive tract were assessed to comprehensively evaluate the magnitude of damage to the ovaries and facilitate comparison between radiation modalities. The uterus responds to changes in hormones secreted by the ovary and as such, was used as a measure of ovarian follicular activity within appropriate time frames. We tested total doses > 6-7 Gy because the sparing effect of FLASH-RT on normal tissues has been predominantly described above this range.[2] Considering radiation sensitivity by follicular type as well as follicular maturation time, a dose of 8 Gy was used to evaluate the effect of UHDR-RT on early follicular stages with protracted evaluation of uterine changes, whereas a dose of 16 Gy was used to assess toxicity of FLASH on mature follicles and its immediate impact on uterine weigh and histopathology. Taken together, the data presented here demonstrated that UHDR- and CONV-RT damaged ovarian follicles similarly.

The applicability of FLASH-RT in clinical settings could be limited if only doses above 7 Gy were able to confer normal tissue sparing. Few studies have evaluated the protective effect of UHDR-RT at doses relevant to fractionated or hypofractionated regimens currently used clinically.[15,16,40] To this end, we evaluated the biological impact of a dose of 5 Gy on the mouse testis. Radiation-induced killing of germ cells translates into decreased testicular weights which were used in this study as a quantitative readout of

radiation-induced toxicity. Due to the exquisite radiation sensitivity of spermatogenic germ cells, this dose was selected in order to allow survival of some spermatogonia and subsequent evaluation of tubular repopulation. Our data from organ weights along with the percent of degenerate seminiferous tubules demonstrated that UHDR- and CONV-RT caused comparable damage to germ cells and the seminiferous epithelium overall.

Male and female germ cells are among the most radiation sensitive cell types in the body along with progenitor cells of the intestinal epithelium, hematopoietic progenitors and lymphocytes.[24] The extreme radiosensitivity of some of these cell types, such as the intestinal epithelial, spermatogenic and marrow cell lines is linked to their high proliferation rates whereas in other cases, namely oocytes and lymphocytes, the reason for this extreme sensitivity is not fully understood.[23] Our results indicating a lack of sparing of UHDR-RT on the gonads of mice is not entirely unexpected as previous studies focusing on other highly radiation sensitive tissues have either failed to demonstrate an effect or have shown effects of a smaller magnitude than those observed in less radiosensitive tissues. For instance, Venkatesulu et al investigated the effect of single and fractionated UHDR-RT in mouse models of radiation-induced lymphopenia and reported equal depletion of lymphocytes between UHDR- and CONV-RT.[16] Chabi et al analyzed the impact of FLASH-RT on human hematopoietic progenitor cells in mice with and without leukemia. Depending on the model, a spectrum of outcomes ranging from milder to more severe toxicity of FLASH-RT was observed following total body irradiation.[15] Similarly, the reported effects of FLASH-RT on mouse models of intestinal toxicity range from preventing death after a traditionally lethal dose of radiation to increasing severity of gastrointestinal syndrome and decreased survival.[13,16] Intriguingly, a number of studies

have shown modest increases in intestinal crypt survival acutely, but whether these changes had an impact on the clinical severity of gastrointestinal syndrome was not reported (e.g., body weight changes and overall survival).[41]

Differences in irradiation beam parameters used across different institutions are thought to be a major contributor to the conflicting experimental results of FLASH regarding normal tissues effects. In an effort to mitigate these issues, recommendations on critical physical parameters as well as standards for uniformly reporting physical aspects of FLASH have been made.[22] One limitation of the present study is the inability to assess the effect of dose rate as an independent variable as the irradiation device used herein operates at discrete pulse repetition frequencies and pulse widths, and dose and dose rate are interdependent. Nonetheless, it should be emphasized that doses, dose rates (mean and instantaneous) and overall treatment times used in our study were kept within recommended ranges in all experiments. In addition, we thoroughly report beam parameter details and provide information on prescribed dose and corresponding dosimetry, thus demonstrating that the suggested optimal beam delivery conditions to trigger the FLASH effect were met. Another potential limitation of this study is the relatively low number of mice used. However, the low intra-group variability in organ weights and histological findings as well as a high level of consistency of results between replicated experiments support the significance of the findings.

CONCLUSIONS

To the best of our knowledge, this is the first study evaluating the impact of UHDR-RT on healthy gonadal tissues of mice. Our data suggest that the short-term effects of UHDR-

RT on the mouse gonads are comparable to those of CONV-RT. This study extends and complements the current knowledge on the effects of FLASH-RT on acutely responding tissues and reinforces the notion that not all UHDR radiation will universally decrease toxicity to healthy tissues. In addition, our inability to trigger normal tissue protection using FLASH-RT despite adhering to recommendations and best practices concerning its main physical aspects attests to the complexity of this phenomenon and the need for further investigation.

Declaration of interests

The authors declare the following financial interests/personal relationships which may be considered as potential competing interests:

Arnab Chakravarti reports a relationship with Varian Medical Systems that includes: funding grants. Dukagjin Blakaj reports a relationship with IntraOp Medical that includes: funding grants. Ashley Cetnar reports a relationship with AAPM Rocky Mountain Chapter Meeting that includes: travel reimbursement. Ashley Cetnar reports a relationship with American Association of Physicist in Medicine that includes: board membership. Joseph P. McElroy reports a relationship with The Ohio State University Department of Radiation Oncology that includes: employment and non-financial support. Jessica Fleming serves as Associate Senior Editor for Advances in Radiation Oncology. Ahmet Ayan serves as Associate Section Editor for Advances in Radiation Oncology.

REFERENCES

1. Seminars in Radiation Oncology | Normal Tissue Injury | ScienceDirect.com by Elsevier. Accessed June 21, 2022. https://www.sciencedirect.com/journal/seminars-in-radiation-oncology/vol/27/issue/4

2. Kacem H, Almeida A, Cherbuin N, Vozenin MC. Understanding the FLASH effect to unravel the potential of ultra-high dose rate irradiation. *Int J Radiat Biol*. 2022;98(3):506-516. doi:10.1080/09553002.2021.2004328/SUPPL_FILE/IRAB_A_2004328_SM8161.XLSX

3. Hughes JR, Parsons JL. FLASH Radiotherapy: Current Knowledge and Future Insights Using Proton-Beam Therapy. *International Journal of Molecular Sciences 2020, Vol 21, Page 6492*. 2020;21(18):6492. doi:10.3390/IJMS21186492

4. Friedl AA, Prise KM, Butterworth KT, Montay-Gruel P, Favaudon V. Radiobiology of the FLASH effect. *Med Phys*. 2022;49(3):1993-2013. doi:10.1002/MP.15184

5. Vorhees C v., Vatner RE, Williams MT. Review of Conventional and High Dose Rate Brain Radiation (FLASH): Neurobehavioural, Neurocognitive and Assessment Issues in Rodent Models. *Clin Oncol*. 2021;33(11):e482-e491. doi:10.1016/J.CLON.2021.09.002

6. Favaudon V, Caplier L, Monceau V, et al. Ultrahigh dose-rate FLASH irradiation increases the differential response between normal and tumor tissue in mice. *Sci Transl Med*. 2014;6(245). doi:10.1126/SCITRANSLMED.3008973

7. Simmons DA, Lartey FM, Schüler E, et al. Reduced cognitive deficits after FLASH irradiation of whole mouse brain are associated with less hippocampal dendritic spine loss and neuroinflammation. *Radiotherapy and Oncology*. 2019;139:4-10. doi:10.1016/J.RADONC.2019.06.006

8. Fouillade C, Curras-Alonso S, Giuranno L, et al. FLASH irradiation spares lung progenitor cells and limits the incidence of radio-induced senescence. *Clinical Cancer Research*. 2020;26(6):1497-1506. doi:10.1158/1078-0432.CCR-19-1440/75331/AM/FLASH-IRRADIATION-SPARES-LUNG-PROGENITOR-CELLS-AND

9. Soto LA, Casey KM, Wang J, et al. FLASH irradiation results in reduced severe skin toxicity compared to conventional-dose-rate irradiation. *Radiat Res*. 2020;194(6):618-624. doi:10.1667/rade-20-00090

10. Velalopoulou A, Karagounis I v, Cramer GM, et al. FLASH Proton Radiotherapy Spares Normal Epithelial and Mesenchymal Tissues While Preserving Sarcoma Response. doi:10.1158/0008-5472.CAN-21-1500

11. Cunningham S, McCauley S, Vairamani K, et al. FLASH Proton Pencil Beam Scanning Irradiation Minimizes Radiation-Induced Leg Contracture and Skin Toxicity in Mice. *Cancers 2021, Vol 13, Page 1012*. 2021;13(5):1012. doi:10.3390/CANCERS13051012

12. Vozenin MC, de Fornel P, Petersson K, et al. The Advantage of FLASH Radiotherapy Confirmed in Mini-pig and Cat-cancer Patients. *Clinical Cancer Research*. 2019;25(1):35-42. doi:10.1158/1078-0432.CCR-17-3375/274517/AM/THE-ADVANTAGE-OF-FLASH-RADIOTHERAPY-CONFIRMED-IN

13. Levy K, Natarajan S, Wang J, et al. Abdominal FLASH irradiation reduces radiation-induced gastrointestinal toxicity for the treatment of ovarian cancer in

mice. *Scientific Reports 2020 10:1*. 2020;10(1):1-14. doi:10.1038/s41598-020-78017-7

14. Ruan JL, Lee C, Wouters S, et al. Irradiation at Ultra-High (FLASH) Dose Rates Reduces Acute Normal Tissue Toxicity in the Mouse Gastrointestinal System. *International Journal of Radiation Oncology*Biology*Physics*. 2021;111(5):1250-1261. doi:10.1016/J.IJROBP.2021.08.004

15. Chabi S, To TH van, Leavitt R, et al. Ultra-high-dose-rate FLASH and Conventional-Dose-Rate Irradiation Differentially Affect Human Acute Lymphoblastic Leukemia and Normal Hematopoiesis. *Int J Radiat Oncol Biol Phys*. 2021;109(3):819-829. doi:10.1016/J.IJROBP.2020.10.012/ATTACHMENT/48F42B74-EC77-4E2E-BDD5-CB2EC3B932BC/MMC2.PPTX

16. Venkatesulu BP, Sharma A, Pollard-Larkin JM, et al. Ultra high dose rate (35;Gy/sec) radiation does not spare the normal tissue in cardiac and splenic models of lymphopenia and gastrointestinal syndrome. *Sci Rep*. 2019;9(1). doi:10.1038/S41598-019-53562-Y

17. Bley CR, Wolf F, Gonçalves Jorge P, et al. Dose- and Volume-Limiting Late Toxicity of FLASH Radiotherapy in Cats with Squamous Cell Carcinoma of the Nasal Planum and in Mini Pigs. *Clinical Cancer Research*. Published online April 29, 2022:OF1-OF10. doi:10.1158/1078-0432.CCR-22-0262

18. Gaide O, Herrera F, Sozzi WJ, et al. Comparison of ultra-high versus conventional dose rate radiotherapy in a patient with cutaneous lymphoma.

Radiotherapy and Oncology. Published online January 5, 2022. doi:10.1016/J.RADONC.2021.12.045

19. Beyreuther E, Brand M, Hans S, et al. Feasibility of proton FLASH effect tested by zebrafish embryo irradiation. *Radiother Oncol*. 2019;139:46-50. doi:10.1016/J.RADONC.2019.06.024

20. Small KL, Henthorn NT, Angal-Kalinin D, et al. Evaluating very high energy electron RBE from nanodosimetric pBR322 plasmid DNA damage. *Scientific Reports* |. 2021;11:3341. doi:10.1038/s41598-021-82772-6

21. Perstin A, Poirier Y, Sawant A, Tambasco M. Physics Contribution Quantifying the DNA-damaging Effects of FLASH Irradiation With Plasmid DNA. Published online 2022. doi:10.1016/j.ijrobp.2022.01.049

22. Schüler E, Acharya M, Montay-Gruel P, Loo BW, Vozenin MC, Maxim PG. Ultra-high dose rate electron beams and the FLASH effect: From preclinical evidence to a new radiotherapy paradigm. *Med Phys*. 2022;49(3):2082-2095. doi:10.1002/MP.15442

23. McBride WH, Schaue D. Radiation-induced tissue damage and response. *Journal of Pathology*. 2020;250(5):647-655. doi:10.1002/PATH.5389

24. Rubin P, Casarett GW. CLINICAL RADIATION PATHOLOGY AS APPLIED T O CURATIVE RADIOTHERAPY. *Cancer*. 1968;22(4):767-778. doi:10.1002/1097-0142

25. Nicholas S, Chen L, Choflet A, et al. Pelvic Radiation and Normal Tissue Toxicity. *Semin Radiat Oncol*. 2017;27(4):358-369. doi:10.1016/J.SEMRADONC.2017.04.010

26. Nakayama K, Milbourne A, Schover LR, Champlin RE, Ueno NT. Gonadal failure after treatment of hematologic malignancies: from recognition to management for health-care providers. *Nat Clin Pract Oncol*. 2008;5(2):78-89. doi:10.1038/NCPONC1016

27. Koch A, Gulani J, King G, Hieber K, Chappel M, Ossetrova N. Establishment of Early Endpoints in Mouse Total-Body Irradiation Model. *PLoS One*. 2016;11(8). doi:10.1371/JOURNAL.PONE.0161079

28. Al-Jamal JH, Dubin NH. The effect of raloxifene on the uterine weight response in immature mice exposed to 17beta-estradiol, 1,1,1-trichloro-2, 2-bis(p-chlorophenyl)ethane, and methoxychlor. *Am J Obstet Gynecol*. 2000;182(5):1099-1102. doi:10.1067/MOB.2000.105407

29. McClellan KA, Gosden R, Taketo T. Continuous loss of oocytes throughout meiotic prophase in the normal mouse ovary. *Dev Biol*. 2003;258(2):334-348. doi:10.1016/S0012-1606(03)00132-5

30. Adriaens I, Smitz J, Jacquet P. The current knowledge on radiosensitivity of ovarian follicle development stages. *Hum Reprod Update*. 2009;15(3):359-377. doi:10.1093/HUMUPD/DMN063

31. Eppig JJ, Wigglesworth K, Pendola FL. The mammalian oocyte orchestrates the rate of ovarian follicular development. *Proc Natl Acad Sci U S A*.

2002;99(5):2890-2894. doi:10.1073/PNAS.052658699/ASSET/1EC75557-3410-4DC0-B4A3-052CB5B6AEB0/ASSETS/GRAPHIC/PQ0526586005.JPEG

32. Zheng W, Zhang H, Liu K. The two classes of primordial follicles in the mouse ovary: their development, physiological functions and implications for future research. *Mol Hum Reprod*. 2014;20(4):286-292. doi:10.1093/MOLEHR/GAU007

33. de Felice F, Marchetti C, Marampon F, Cascialli G, Muzii L, Tombolini V. Radiation effects on male fertility. *Andrology*. 2019;7(1):2-7. doi:10.1111/ANDR.12562

34. MONESI V. Relation between x-ray sensivity and stages of the cell cycle in spermatogogonia of the mouse. *Radiat Res*. 1962;17:809-838. doi:10.2307/3571315

35. Hess RA, de Franca LR. Spermatogenesis and cycle of the seminiferous epithelium. *Adv Exp Med Biol*. 2008;636:1-15. doi:10.1007/978-0-387-09597-4_1

36. Dixon D, Alison R, Bach U, et al. Nonproliferative and proliferative lesions of the rat and mouse female reproductive system. *J Toxicol Pathol*. 2014;27(3-4 Suppl). doi:10.1293/TOX.27.1S

37. Westwood FR. The female rat reproductive cycle: a practical histological guide to staging. *Toxicol Pathol*. 2008;36(3):375-384. doi:10.1177/0192623308315665

38. Creasy D, Bube A, de Rijk E, et al. Proliferative and nonproliferative lesions of the rat and mouse male reproductive system. *Toxicol Pathol*. 2012;40(6 Suppl). doi:10.1177/0192623312454337

39. Jeruss JS, Woodruff TK. Preservation of Fertility in Patients with Cancer. *https://doi.org/101056/NEJMra0801454*. 2009;360(9):902-911. doi:10.1056/NEJMRA0801454

40. Montay-Gruel P, Acharya MM, Jorge PG, et al. Hypofractionated FLASH-RT as an Effective Treatment against Glioblastoma that Reduces Neurocognitive Side Effects in Mice. *Clin Cancer Res*. 2021;27(3):775-784. doi:10.1158/1078-0432.CCR-20-0894

41. Ruan JL, Lee C, Wouters S, et al. Irradiation at Ultra-High (FLASH) Dose Rates Reduces Acute Normal Tissue Toxicity in the Mouse Gastrointestinal System. *Int J Radiat Oncol Biol Phys*. 2021;111(5):1250-1261. doi:10.1016/J.IJROBP.2021.08.004

FIGURE LEGENDS

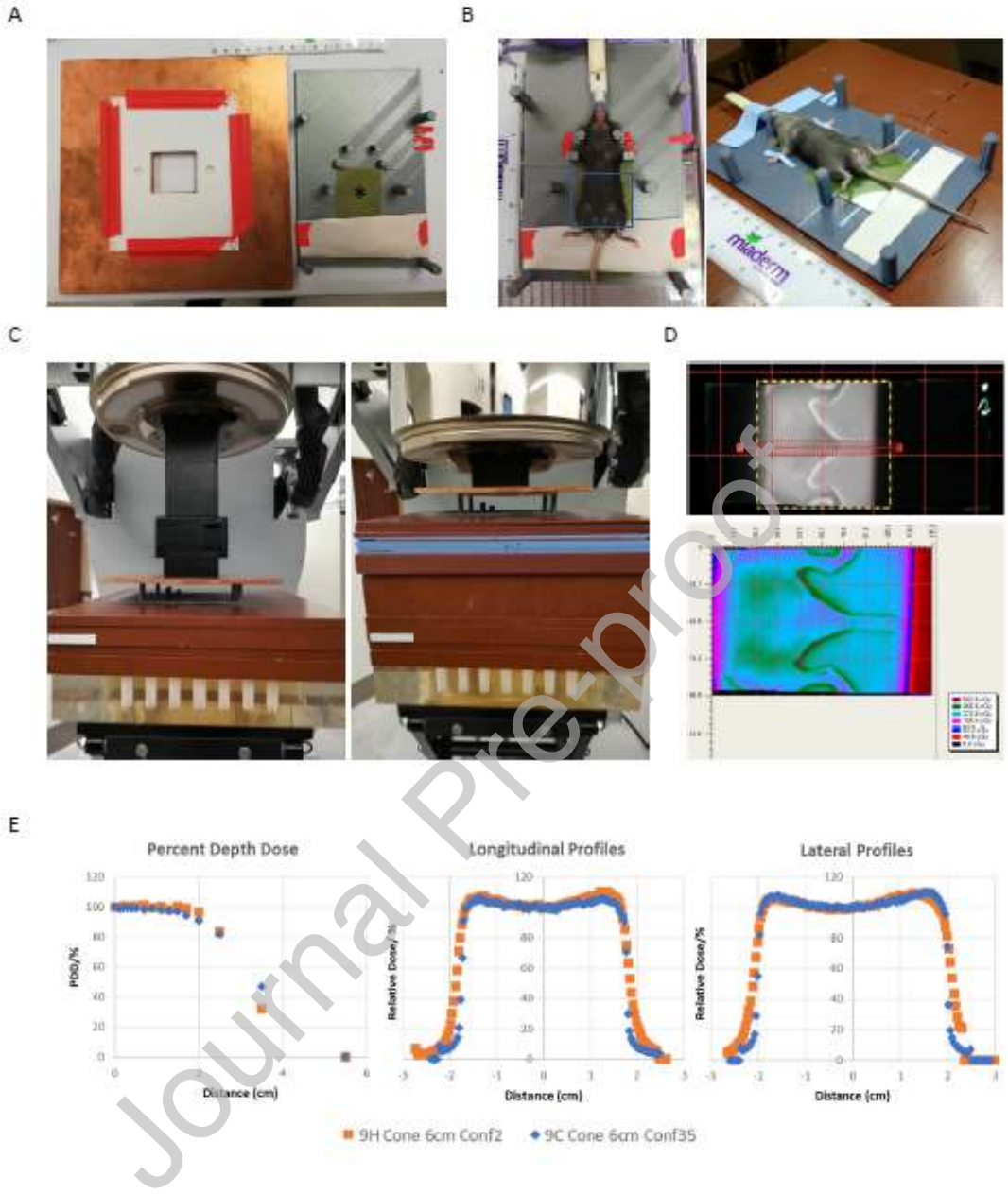

Figure 1. Mouse irradiation setup. (A) Plastic immobilization device comprised of a base (right) and a top piece secured to a copper collimator (left). A 3.5x4 cm^2 opening within the top piece ensures reproducible placement of the collimator. (B) Plastic immobilization device holding an anesthetized mouse (left) prior to securing the copper collimator. The blue outline on left panel indicates the placement of the 3.5x4 cm abdominal irradiation

field (female). The red laser pointer on right panel area indicates the center of the 3.5x4 cm^2 pelvic irradiation field (male). GafChromic film (* in A) was placed underneath the mouse for exit dosimetry. (C) Fully assembled immobilization device and setup configurations for CONV (left) or UHDR (right) irradiation. (D) Example of an exit dosimetry film (top) and corresponding isodose map (bottom) on the pelvic region of a male mouse. (E) Percent depth dose as well as longitudinal and lateral dose profiles acquired at d_{max} using GafChromic film in solid water phantom slabs.

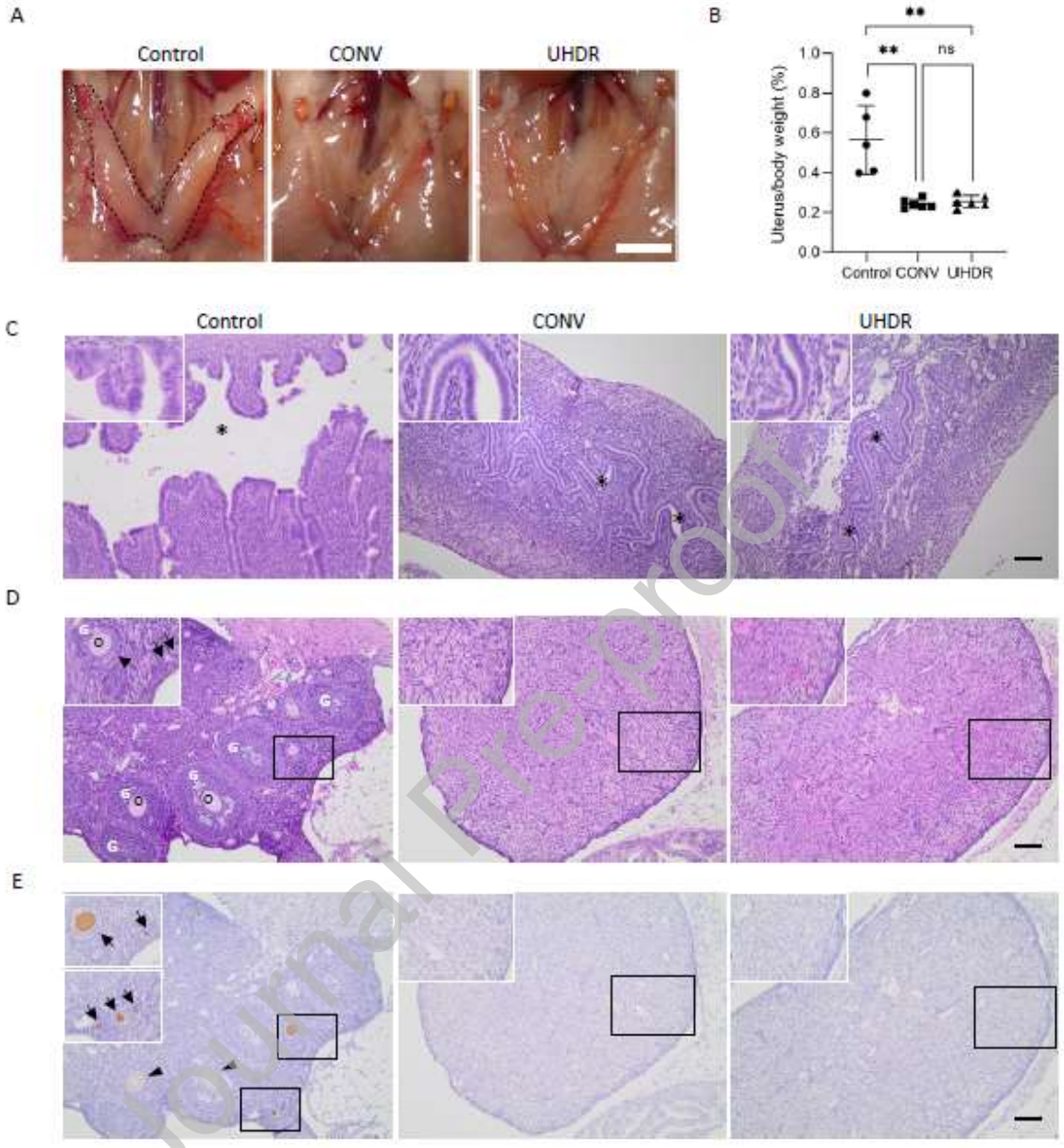

Figure 2. Effect of CONV- or UHDR-RT on the reproductive tract of female mice 2 months after receiving 8 Gy to the abdomen. (A) Macroscopic appearance of uteri and ovaries (indicated within dashed lines on control) Scale bar: 5 mm (B) Uterine weights. Data are presented as mean ± SD; n = 5-6 mice per group; ns, P > 0.05; **, P Ò0.01. (C) H&E-stained sections of uteri. Lumen (asterisks) was narrow in CONV/UHDR-irradiated uteri.

Insets: higher magnification of surface epithelium. Tall columnar epithelium with necrotic debris (hormonally induced) is shown in control (D) H&E-stained sections of ovaries. Normal follicles of different sizes composed of an oocyte (O) and surrounding granulosa cells (G) are apparent in control ovaries [smaller follicles (arrows) are magnified in inset]. Follicles of all types are lacking in CONV/UHDR-irradiated ovaries which are composed of sheets of round cells (magnified in insets). (E) MVH immunostaining of ovaries. Brown cytoplasmic staining highlights oocytes within follicles. Insets: higher magnification of boxed areas showing normal follicles of different types in control ovaries (arrows and arrowheads) and the lack of follicles of all types in CONV/UHDR-irradiated ovaries. Note that the more mature oocytes in tertiary follicles stain faintly (arrowhead). Scale bars: 50 microns.

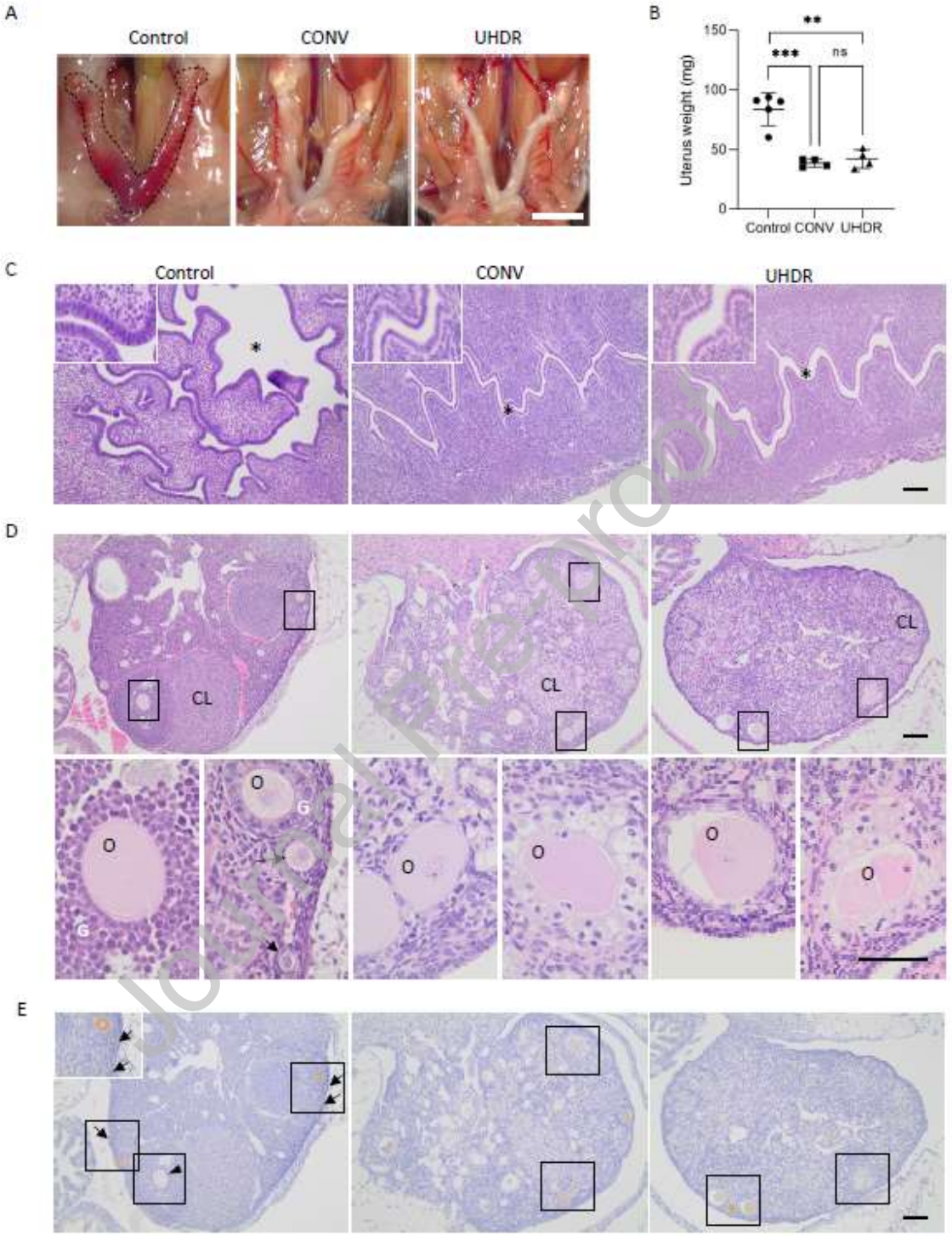

Figure 3. Effect of CONV- or UHDR-RT on the reproductive tract of female mice 6 days after receiving a dose of 16 Gy to the abdomen (A) Macroscopic appearance of uteri and ovaries (indicated within dashed lines on control). Scale bar: 5 mm (B) Uterine weights. Data are presented as mean ± SD; n = 4-5 mice per group; ns, P > 0.05; **, P Ò0.01 ***, P Ò 0.001. (C) H&E-stained sections of uteri. The lumen (asterisks) was narrow in CONV/UHDR-irradiated uteri. Insets: higher magnification of surface epithelium. Tall columnar epithelium with mitotic figures (hormonally induced) is shown in control. (D) H&E-stained sections of ovaries. Intact follicles (boxes in control) or remnants of follicles (boxes in CONV/UHDR-irradiated ovaries) are shown at higher magnification on bottom panels. Intact follicles are composed of oocytes (O) and granulosa cells (G). Remnants of follicles contain oocytes [presumably non-degenerate (left) and degenerate (right)] and lack granulosa cell layers. Small follicles [small oocyte and single layer of granulosa cells (arrows)] are only found in control ovaries. Only remnants of corpora lutea (CL) are visible in CONV/UHDR-irradiated ovaries. (E) MVH immunostaining of ovaries. Brown cytoplasmic staining highlights oocytes within intact follicles (boxes in control) or follicle remnants (boxes in CONV/UHDR). Mature oocytes in tertiary follicles stain faintly (arrowhead in control ovary). Oocytes within small follicles (arrows in control) are absent in CONV/UHDR ovaries. Scale bars: 50 microns.

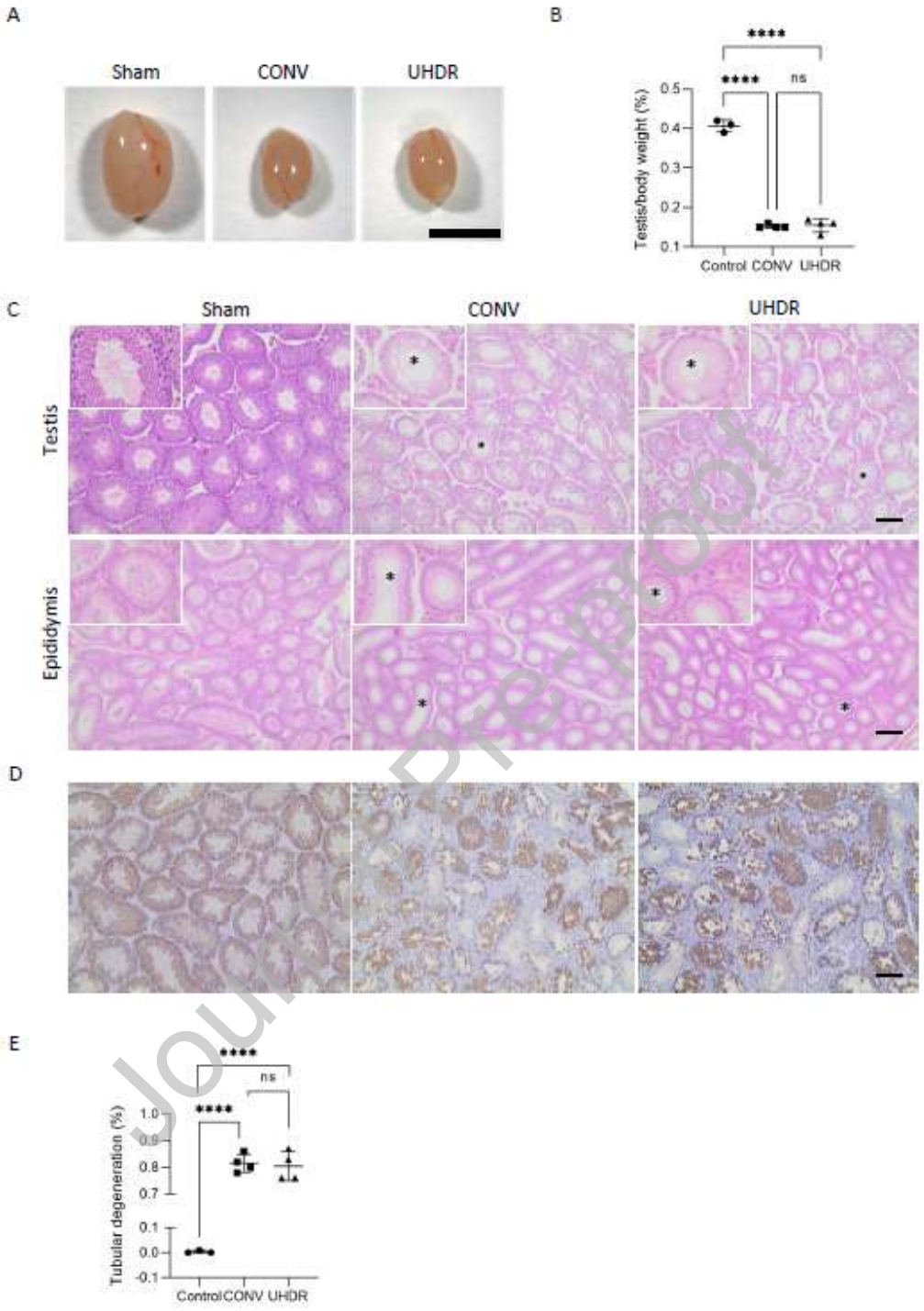

Figure 4. Effect of CONV- or UHDR-RT on the testis of mice 35 days after receiving a dose of 5 Gy to the pelvis. (A) Macroscopic appearance of testis. Scale bar: 5 mm (B)

Testis weight. (C) H&E-stained sections of testis and epididymis. Asterisks indicate examples of seminiferous tubules that are completely devoid germ cells (magnified in insets on CONV/UHDR testes) as well as the lack of spermatozoa within the epididymis in CONV/UHDR testes. Spermatozoa are present in magnified inset on control. (D) MVH immunostaining of testis highlights reduction in germ cell numbers in irradiated testes. (E) Percent of seminiferous tubules exhibiting degenerative changes. Data in (B) and (E) are presented as mean ± SD; n = 3-4 mice per group; ns, P > 0.05; ****, P Ò0.0001. Scale bars: 50 microns.